Scientific
Research
Publishing

A Comparative Study on the Structural and Vibrational Properties of Two Potential Antimicrobial and Anticancer Cyanopyridine Derivatives

María J. Márquez, María B. Márquez, Pablo G. Cataldo, Silvia A. Brandán

Cátedra de Química General, Instituto de Química Inorgánica, Facultad de Bioquímica, Química y Farmacia, Universidad Nacional de Tucumán, Tucumán, Argentina
Email: sbrandan@fbqf.unt.edu.ar

Abstract

2-Hydroxy-4,6-dimethylpyridine-3-carbonitrile and 2-chloro-4,6-dimethylpyridine-3-carbonitrile compounds have been studied from a theoretical point of view in order to know their structural and vibrational properties in gas and aqueous solution phases by means of Density Functional Theory (DFT) calculations. The stable structures in both media were optimized by using the hybrid B3LYP/6-31G* method and the solvent effects in aqueous solution were studied by using the integral equation formalism of the polarizable continuum model (IEFPCM) employing the self-consistent reaction field (SCRF) method. Detailed vibrational analyses for both compounds in the two phases were performed combining the DFT calculations with Pulay's Scaled Quantum Mechanics Force Field (SQMFF) methodology. The different interactions for both compounds were analyzed by means of the bond orders, atomic charges, solvation energies, dipole moments, molecular electrostatic potentials and force constants parameters. The nature of the interactions was studied by using different descriptors.

Keywords

1. Introduction

As part of our investigations on compounds of great pharmacological interest [1], in this work we have studied

from a theoretical point of view the structures and vibrational properties of the 2-hydroxy-4,6-dimethylpyridine-3-carbonitrile and 2-chloro-4,6-dimethylpyridine-3-carbonitrile compounds. These cyanopyridine derivatives play a very important role in the synthesis chemistry organic and, in medicine and pharmacology because these compounds present potential anticancer, antiarrhythmic, anticonvulsant, antiparkinsonian and antimicrobial activities [2]-[8]. Recently, Waly *et al.* have reported the synthesis and antitumor evaluation of some new fused and binary pyridines together with a modified synthetic method for the synthesis of 2-chloro-4,6-dimethyl-nicotinonitrile [2]. In other studies, the synthesis and antiarrhythmic activities of some synthesized pyridine derivatives fused with thiophene ring were also reported while new pyridine derivatives were synthesized and evaluated as analgesic, anticonvulsant and anti-parkinsonian agents [4]. Besides, derivatives as the thieno [2,3-d] pyrimidines can be used to eliminate fungi in plants [9] and to inhibit the growth of cancer cells [10] while some thiopyridines and carbonitrile compounds are also used as insecticides [11]-[13]. All these studies clearly show that the modifications in the pyridine structure by incorporation of different groups and/or rings produce different biochemical behavior and biological activity that are evidenced by different structure-activity relationships (SAR). Hence, the studies of the structural properties of these derivatives are important to predict their reactivities and behavior in different media and systems which are present, especially when these compounds are used as pharmacological drugs for the health human. Furthermore, the knowing of its structures is also very important because it permits their quickly identifications by means of vibrational spectroscopy. So far, the crystal and molecular structures of both compounds were not determined and only the structure of 2-anilino-4,6-dimethylpyridine-3-carbonitrile, an intermediate in the synthesis of 5-aminobenzo [*b*] [1] [8] naphthyridines was published by Mefetah *et al.* [14]. On the other hand, the crystal structure of 4-cyanopyridine was determined by Laing *et al.* [15] from three-dimensional single crystal X-ray data collected by standard film techniques while the structure of the 4-cyanopyridinium dihydrogen phosphate-isonicotinonitrile-phosphoric acid compound was refined by Wang [16] who has determined that this compound has a asymmetric unit because it contains one 4-cyanopyridinium cation, one $H_2PO_4^-$ anion, one independent isonicotinonitrile molecule and one independent H_3PO_4 molecule. Also, from long time the cyano group structure in 3-cyanopyridinium tetrachloroferrate (III)-3-cyanopyridine was determined by Daran *et al.* [17] by X-ray diffraction method. In the present work, we presented the structural and vibrational studies of the 2-hydroxy-4,6-dimethylpyridine-3-carbonitrile and 2-chloro-4,6-dimethylpyridine-3-carbonitrile compounds in order to, 1) determine their theoretical and more stable structures in gas and aqueous solution phases, 2) perform complete assignments of the corresponding infrared and Raman spectra, 3) evaluate their structural properties in gas and aqueous solution phases and, 4) predict the behavior of both molecules in gas and aqueous solution phases by using diverse descriptors [18] [19]. For those purposes, first, both structures were optimized in gas and aqueous solution phases using the hybrid B3LYP/6-31G* method and the solvent effects in aqueous solution were studied by using the self-consistent reaction field (SCRF) calculations with the IEFPCM model [20]. Then, the corresponding frequencies were calculated at the same level of theory in order to perform the complete assignments of all the bands observed in the vibrational spectra combining the natural internal coordinates with the scaled mechanical force field (SQMFF) procedure [21]. Additionally, molecular electrostatic potentials (MEP), highest occupied molecular orbital-lowest unoccupied molecular orbital (HOMO-LUMO) [22], natural bond orbital (NBO) [23] [24] and atoms in the molecules (AIM) [25] [26] calculations were performed in order to evaluate the structural properties such as, electrostatic potentials, atomic charges, bond orders, stabilization energies, topological properties and solvation energies in both media, and to predict the properties of the two compounds in both media. Here, the structural and vibrational properties of both compounds were compared and analyzed.

2. Computational Details

Initially, the structures of the 2-hydroxy-4,6-dimethylpyridine-3-carbonitrile (**2-OH**) and 2-chloro-4,6-dimethylpyridine-3-carbonitrile (**2-Cl**) derivatives were modeled with the *GaussView* program [27] and optimized by using the hybrid B3LYP/6-31G* method [28] [29] employing the Gaussian 09 program [30]. For each (**2-OH**) and (**2-Cl**) derivative only a stable conformation of C_1 symmetry was optimized which can be seen in **Figure 1** together with the labelling of the atoms. In aqueous solution, the solvent effects were simulated employing the SCRF method by using the IEFPCM model [20] with a value of 78.39 to simulate the aqueous medium. This way, the geometrical parameters and frequencies for those derivatives were calculated at the same level of theory in order to confirm the nature of the stationary points. Also, the solvation energies were calculated from the IEFPCM calculations with radii and non-electrostatic terms by using the SMD solvation model [31], as re-
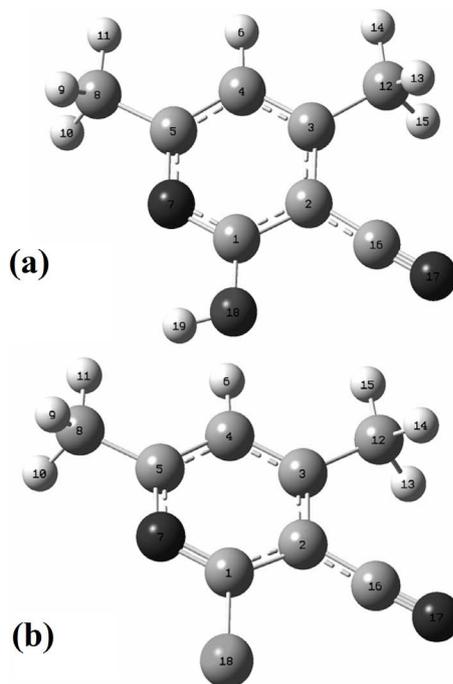
Figure 1. Theoretical structures and atoms numbering for the: (a) 2-Hydroxy-4,6-dimethylpyridine-3-carbonitrile and; (b) 2-Chloro-4,6-dimethylpyridine-3-carbonitrile derivatives.

ported for other molecules in aqueous medium [32]-[34].

For both derivatives, the variations of molecular volumes expressed as a difference between the volumes in aqueous solution in relation to the volume in gas phase were calculated employing the Moldraw program [35]. In order to know the exact nature of the interactions present in both derivatives the atomic charges and those derived from Merz-Kollman were considered in this study [36] together with the corresponding MEP. In addition, the bond orders were calculated at the same theory level from NBO calculations by using the NBO 3.1 program [24], as implemented in the Gaussian 09 package [30]. The different interactions predicted for both derivatives in the two studied media were analyzed by means of calculations of the electronic charge density topological with the AIM2000 program package [26]. The harmonic force fields for both derivatives were evaluated at the same level of theory by using the Molvib program [37] and following the SQMFF procedure [21]. To perform the complete assignments, only the potential energy distribution components (PEDs) ≥10% were considered from the resulting SQM.

3. Results and Discussion

3.1. Geometry

Table 1 show the calculated geometrical parameters for the two studied cyanopyridine derivatives in gas and aqueous solution phases by using the B3LYP/6-31G* level of theory. The theoretical values were compared with the experimental ones determined by Mefetah *et al.* for 2-anilino-4,6-dimethylpyridine-3-carbonitrile by using X-ray diffraction method by means of the root mean square deviation (RMSD) [14]. The results show that for both molecules the calculated bond length and angles values are in agreement with the experimental ones with RSMD values for bond length between 0.004 and 0.005 Å while the difference for the bond angles are between 0.7˚ and 0.8˚. Comparing the calculated parameters for the two derivatives with those experimental obtained for 4-cyanopyridine [15], we observed that the experimental C≡N distance in it derivative is 1.137 Å while in the 4-cyanopyridinium dihydrogen phosphate-isonicotinonitrile-phosphoric acid derivative [16] is 1.142 Å and in 3-cyanopyridinium tetraehloroferrate(lll)-3-cyanopyridine is of 1.102 Å [17].

The results clearly show that this bond is strongly dependent of the groups linked to the pyridine ring and of the position of the C-C≡N group. On the other hand, the C-C bond linked to the C≡N bond in 4-cyanopyridine is

Table 1. Comparison of calculated geometrical parameters for the two studied cyanopyridine derivatives.

Parameter	B3LYP/6-31G*[a]				Exp.[b]
	2-Hydroxy-4,6-dimethylpyridine-3-carbonitrile		2-Chloro-4,6-dimethylpyridine-3-carbonitrile		
	Gas phase	PCM	Gas phase	PCM	
Bond lengths (Å)					
C1-C2	1.412	1.411	1.410	1.405	
C2-C3	1.407	1.409	1.411	1.413	1.383
C3-C12	1.505	1.501	1.505	1.501	1.493
C3-C4	1.397	1.395	1.395	1.394	1.384
C4-C5	1.397	1.397	1.397	1.396	1.383
C5-C8	1.505	1.501	1.504	1.499	1.501
C1-N7	1.325	1.324	1.314	1.312	1.327
C5-N7	1.345	1.350	1.347	1.353	1.346
C2-C16	1.427	1.422	1.428	1.425	1.426
C16-N17	1.164	1.167	1.163	1.166	1.145
C1-O18/C1-Cl18	1.345	1.352	1.754	1.764	
RMSD	0.004	0.004	0.005	0.005	
Bond angles (°)					
C1-C2-C3	117.8	118.3	117.6	117.6	
C2-C3-C4	117.5	117.1	117.3	117.0	121.8
C2-C3-C12	120.7	121.0	120.8	121.0	121.5
C4-C3-C12	121.6	121.8	121.7	121.9	120.0
C4-C5-N7	121.9	122.1	121.6	121.5	
C4-C5-C8	121.8	121.3	122.2	121.8	121.8
C8-C5-N7	116.1	116.5	116.1	116.5	115.2
C2-C1-O18/Cl18	118.3	117.6	119.0	118.8	
N7-C1-O18/Cl18	117.6	118.4	116.4	116.1	
C2-C16-N17	178.1	179.7	177.2	178.6	178.7
C3-C2-C16	121.3	121.6	120.1	120.6	120.0
C1-C2-C16	120.8	119.9	122.2	121.6	
RMSD	0.7	0.8	0.7	0.8	
Dihedral angle (°)					
C1-C2-C16-N17	179.9	179.9	180.0	180.0	
C3-C2-C16-N17	−0.0	−0.0	0.0	0.0	−94.0
C3-C2-C1-O18	180.0	−179.9	180.0	180.0	
C5-N7-C1-O18	−180.0	−179.9	180.0	180.0	
C1-C2-C3-C12	179.9	179.9	180.0	180.0	
C1-N7-C5-C8	−179.9	179.9	180.0	180.0	−179.2
C3-C4-C5-C8	179.9	−180.0	180.0	180.0	179.1
C5-C4-C3-C12	−179.9	−179.9	180.0	180.0	179.1
RMSD	92.7	157.2	92.8	92.8	

[a]This work; [b]From Ref [38].

1.439 Å [15], in 4-cyanopyridinium dihydrogen phosphate-isonicotinonitrile-phosphoric acid [16] is 1.453 Å and in 3-cyanopyridinium tetraehloroferrate (III)-3-cyanopyridine [17] is between 1.452 and 1.480 Å, being the calculated values for (**2-OH**) and (**2-Cl**) between 1.428 and 1.422 Å. Thus, these values indicating that this bond is less depending of the position of the C-C≡N group and of the groups linked to the pyridine ring. Also, in both derivatives we observed that the C1-N7 distances are slightly different from the C5-N7 distances indicating that both pyridinic bonds are dependent of the groups linked to the C1 or C5 atoms belonging to the C-N bonds, these are, in the (**2-OH**) derivative, C1-O18 and C5-CH$_3$ while in the (**2-Cl**) derivative are C1-Cl18 and C5-CH$_3$.

Experimentally, the C-N distance in the symmetric molecule of 4-cyanopyridine [15] is 1.331 Å, in 4-cyanopyridinium dihydrogen phosphate-isonicotinonitrile-phosphoric acid [16] are 1.339 and 1.337 Å and, in 3-cyanopyridinium tetraehloroferrate(III)-3-cyanopyridine [17] those distances are between 1.301 and 1.351 Å. The differences observed in the latter molecule are justified because two molecules are linked in asymmetric form by the N atoms of both pyridine rings. Also, in the (**2-OH**) and (**2-Cl**) derivatives (**Table 1**) the two C-N distances are different because both molecules are asymmetrics. In aqueous solution, we observed that in both derivatives some distances slightly change with the hydration, being more evident in the C1-O18 and C1-Cl18 distances because both are sites of H bonds formation. In the (**2-OH**) derivative, the C-OH site is an electrophilic region while in the (**2-Cl**) derivative the C-Cl site is a nucleophilic region. On the other hand, **Table S1** show a comparison of the total energies and the corresponding dipole moment values for both derivatives in the two media by using the B3LYP/6-31G* method. Note that in both media the dipole moments for the (**2-Cl**) derivative are higher than the other ones, as expected because the Cl atom is a voluminous atom. For this reasons, the calculated molecular volumes for the (**2-Cl**) derivative in both media by using the Moldraw program [35] and the B3LYP/6-31G* method are higher than the other ones, as observed in **Table 2**. In the (**2-Cl**) derivative, clearly there is a volume contraction with the hydration while in the (**2-OH**) derivative is observed a volume expansion, in agreement with the solvation energies values, as can be seen in **Table 2**.

3.2. Solvation Energies

The uncorrected solvation energies (ΔG_u), calculated as relative energies (ΔE) and defined as the difference between the total energies in aqueous solutions and the values in gas phase for the (**2-OH**) and (**2-Cl**) derivatives using the 6-31G* basis set, are presented in **Table 2**. Here, the uncorrected (ΔG_u) and corrected (ΔG_c) solvation energies together with the total non electrostatic terms (ΔG_{ne}) due to the cavitation, dispersion and repulsion energies were calculated by using the PCM/SMD model [31], in form similar as reported for other molecules in aqueous solution [32]-[34]. Note that for the (**2-OH**) derivative a higher ΔG_c value is obtained, probably due to its higher variation of volume in solution (**Table 2**), for this reason, a higher hydration is expected for this derivative in aqueous solution.

3.3. Molecular Electrostatic Potential, Atomic Charges and Bond Orders

The molecular electrostatic potential values for both derivatives calculated in the two media by using the B3LYP/6-31G* method are given in **Table S2**. In (**2-OH**), the most negatives molecular electrostatic potential values are observed on the N7, N17 and O18 atoms and the less negative on the H19 atom belonging to the OH group while in (**2-Cl**), the most negatives values are observed on the N7, N17 and Cl18 atoms and the less negative on the H atoms. Note that in both molecules the N17 atom have higher values than the N7 ones, for these reasons, strong red colorations are observed on the surfaces mapped of both derivatives, as observed in **Figure S1**, indicating in both derivatives those regions reacting with potential biological electrophiles. These colorations indicate probably capability of hydrogen bond formation with share of nitrogen atoms of the C≡N or, in aqueous solution through hydrogen atom of -OH moiety. On the contrary, on the H19 atom a strong blue coloration is observed on the surfaces mapped of (**2-OH**) being this region reacting with potential biological nucleophiles. Another important result is the lower molecular electrostatic potential values observed on the H atoms of both

Table 2. Calculated volume and solvation energies (ΔG) for the two studied cyanopyridine derivatives.

B3LYP/6-31G^{*a}					
2-Hydroxy-4,6-dimethylpyridine-3-carbonitrile			2-Chloro-4,6-dimethylpyridine-3-carbonitrile		
Volume (Å^3)					
Gas phase	PCM	ΔV	Gas phase	PCM	ΔV
162.5	163.0	0.5	171.5	171.3	−0.2
Solvation energies (kJ/mol)					
ΔG_u	−32.26	ΔG_{uncorr}	−23.61	ΔG_u	−32.26
$\Delta G_{Totalne}$	19.02	ΔG_{ne}	16.01	$\Delta G_{Totalne}$	19.02
ΔG_c	−13.24	$\Delta G_{corrected}$	−7.6	ΔG_c	−13.24

$\Delta G_c = \Delta G_{uncorrected}{}^{\#} - \Delta G_{Totalnon\ electrostatic}$; [a]This work.

CH$_3$ groups in the chlorinated derivative in the two media in relation to the other one. These results justify the higher blue coloration on the surface mapped of those groups in the chlorinated derivative, as observed in **Figure S1**. In the (**2-OH**) derivative is expected a high reactivity due to the higher proximity between the N17 and O18 atoms (higher repulsion), whose distances in gas and aqueous solution phase are respectively of 3.559 and 3.496 Å while in the chlorinated derivative the N17-Cl18 distances in gas and aqueous solution phases are respectively of 3.743 and 3.698 Å. Note that in aqueous solution increase the reactivities of both derivatives due to the shortening in the distances between both involved atoms. The atomic charges derived from the ESPs (MK) [36] and the NPA charges by using the B3LYP/6-31G* method were calculated for both derivatives in the two media, as can be seen in **Table S3**. The two charges show that despite the only difference between both derivatives are the presence of the OH group and the Cl atom the values are strongly dependent of the groups linked to the pyridine ring and of the position of the C-C≡N group, as was also observed in the Section 3.1. These charges analysis also show that the (**2-OH**) derivative is less stable than the other one due to the higher charge values on the N17 and O18 atoms. Moreover, the different charge values observed on the N7, N17, O18 and Cl18 atoms suggest for the two derivatives a different hydration in solution. The bond orders expressed by Wiberg's indexes for the two derivatives in both media are observed in **Table S4**. Note that the change of the OH group in (**2-OH**) by the Cl atom in (**2-Cl**) increase the bond order values for the N7, N17 and all the C atoms of the pyridine ring while decrease the bond order values of the H and C atoms belonging to the two CH$_3$ groups, thus, the pyridine ring has in gas phase a higher stability in the chlorinated derivative than the other one. Note that the bond order values in both derivatives practically not change in aqueous solution and only a little decreasing is observed in the bond order corresponding to the Cl atom with the hydration. This fact, in (**2-Cl**) is probably related with the contraction volume observed in aqueous solution.

3.4. NBO Analysis

The stability of both derivatives were studied by means of second order perturbation energies E$^{(2)}$ (donor → acceptor) whose values are given in **Table S5**. Here, we considered only those contributions higher than 20 kJ/mol. These results for the (**2-OH**) and (**2-Cl**) derivatives show three different contributions to the total stabilization energies, which are, the $\Delta ET_{\pi \to \pi^*}$, $\Delta ET_{LP \to \sigma^*}$ and $\Delta ET_{\sigma^* \to \sigma^*}$ charges transfer, being the two latter interactions higher in the (**2-OH**) derivative than the other one while, the π-π interactions in the pyridine ring are higher in the chlorinated derivative. These results show that the calculated total stabilization energy favours to the (**2-OH**) derivative revealing thus a higher stability for this derivative in gas and aqueous solution phases. Here, it is very important to note that in the (**2-OH**) derivative the significant increase in the delocalization values in aqueous solution is related with the increase of the C-C and C-N double bonds of the pyridine ring as consequence of the hydration. This way, this analysis shows clearly that the $\Delta ET_{\pi-\pi}$ interactions in the pyridine ring are higher in the chlorinated derivative and in both media while, in general, the ΔE_{Total} are higher in the (**2-OH**) derivative than the other one.

3.5. AIM Study

Both derivatives were also studied employing the AIM analysis [25] [26]. For the (**2-OH**) and (**2-Cl**) derivatives, the charge electron densities, (ρ) and the Laplacian of the electron densities, $\nabla^2\rho(r)$ were calculated for the ring critical points (RCPs) belonging to the pyridine rings and the values can be seen in **Table S6**. The results show higher values in the topological properties for the chlorinated derivative and, also a slightly difference for this derivative with the hydration. Thus, the analysis clearly shows a higher stability for the pyridine ring of the chlorinated derivative in both media, contrarily to that result obtained by NBO analysis.

3.6. Descriptors for Both Derivatives

Many cyanopyridine derivatives have potentials antimicrobial and anticancer activities, for this reason, and to determine the exact nature of the interactions with electrophones and/or nucleophiles and, also to predict the behavior of both derivatives in gas and aqueous solution phases are very important the calculations of some descriptors. If both derivatives are used for the drugs design, the knowledge of these descriptors helps to understand the structural, dynamical, and functional properties of each derivative in both media. Thus, for both derivatives, the HOMO and LUMO orbitals, energy band gap, chemical potential (μ), electro negativity (χ), global

hardness (η), global softness (S) and global electrophilicity index (ω) descriptors [18] [19] were calculated. These descriptors calculated in both phases at B3LYP/6-31G* level of theory can be seen in **Table S7**. Comparing first the energy band gaps between both derivatives we observed that the chlorinated derivative has the highest values in both media indicating a higher stability for this molecule than the other one. Note that the OH group in the pyridine ring generate the reduction of the HOMO-LUMO gap indicating that in the (**2-OH**) derivative that group deactivating the ring and diminishing its potency when it is used as a drug. On the contrary, the presences of a Cl atom in the pyridine ring in (**2-Cl**) compared with (**2-OH**), active that ring and increase its potency. Comparing the calculated chemical hardness η, chemical potential μ and global electrophilicity index ω values for (**2-OH**) with those obtained for (**2-Cl**) in both phases, we observed that (**2-Cl**) is more stable in both media (larger η) and has better capability to accept electrons (bigger electrophilicity index) than (**2-OH**) but, on the contrary, (**2-OH**) is better electrons donor than (**2-Cl**). Here, the lowest molecular electrostatic potentials observed on the H atoms of both CH$_3$ groups for the chlorinated derivative support the better capability to accept electrons while, the highest molecular electrostatic potentials observed on the N7 and N17 atoms of (**2-OH**) suggest that it derivative is better electrons donor than (**2-Cl**).

3.7. NMR Analysis

Experimental and calculated chemical shifts with the GIAO method using 6-311++G** basis set for the ^{1}H and ^{13}C nuclei of both derivatives are compared in **Table S8** and **Table S9** respectively. In general, the calculated shifts for the ^{13}C nuclei are lower than the corresponding experimental values. Note that the calculated chemical shifts for the H nuclei of (**2-OH**) show a significant variation (0.81 ppm) than the (**2-Cl**) derivative (0.22 ppm), in relation to the corresponding experimental values [2]. Probably, the theoretical calculations do not correctly predict the hydrogen chemical shift of the H19 nucleus belonging to the OH group of (**2-OH**), as observed in **Table S8**, because that group is involved in intermolecular H-bonds. Thus, the higher hydration of this derivative is supported by the higher solvation energy in aqueous solution. **Table S9** show that the calculated ^{13}C chemical shifts for both derivatives are slightly different between them, as expected due to the different (OH and Cl groups) present in each structure.

4. Vibrational Analysis

The recorded infrared spectra for both derivatives in solid phase compared with the corresponding theoretical in gas and aqueous solution phases can be seen respectively in **Figure 2** and **Figure 3**. Both infrared spectra in solid phase were taken from Refs [38] [39]. The predicted Raman spectra calculated using B3LYP/6-31G* method for (**2-OH**) and (**2-Cl**) can be seen in **Figure 4**. The (**2-OH**) and (**2-Cl**) derivatives have respectively 51 and 48 normal vibration modes, all active in the infrared and Raman spectra. The experimental and calculated wavenumbers for both derivatives together with the corresponding assignments are shown in **Table 3**. The vibrational assignments of the experimental bands to the normal vibration modes for both derivatives are based on the comparisons with related molecules [40]-[42] and with the results of the calculations performed here. In this work, we presented only the calculations for both derivatives in gas phase because the experimental spectra were not registered. The comparison between the theoretical infrared spectra for (**2-OH**) and (**2-Cl**) using B3LYP functional and 6-31G* basis in gas (black color) and aqueous solution phases (red color) can be seen in **Figure S2**. Note that in both spectra in aqueous solution are observed a shifting and intensification of the bands specially those assigned to the C≡N, C-N, O-H stretchings and in the 1500 - 500 cm^{-1} region attributed to the H bonds, as observed in **Figure S2**. The SQM force fields for both derivatives can be obtained at request. The discussion of assignments of the most important groups for both derivatives is presented as follows.

4.1. Assignments for 2-Hydroxy-4,6-dimethylpyridine-3-carbonitrile

OH modes. The broad and intense band in the IR spectrum of (**2-OH**) centred at 3350 cm^{-1} and predicted in aqueous solution at 3523 cm^{-1}, is assigned to the O-H stretching as observed in compounds containing this group [34] [41]-[44]. The OH in plane deformation mode is assigned to the strong band at 1225 cm^{-1} while the corresponding out-of-plane deformation mode is associated to the band at 495 cm^{-1}.

CH$_3$ modes. The IR bands between at 2980 and 2850 cm^{-1} are assigned to the CH$_3$ antisymmetric and symmetric stretching modes while the bands between 1465 and 1360 cm^{-1} are clearly assigned to the ant symmetric and symmetric CH$_3$ deformation modes. The four expected rocking modes are assigned to the shoulder and
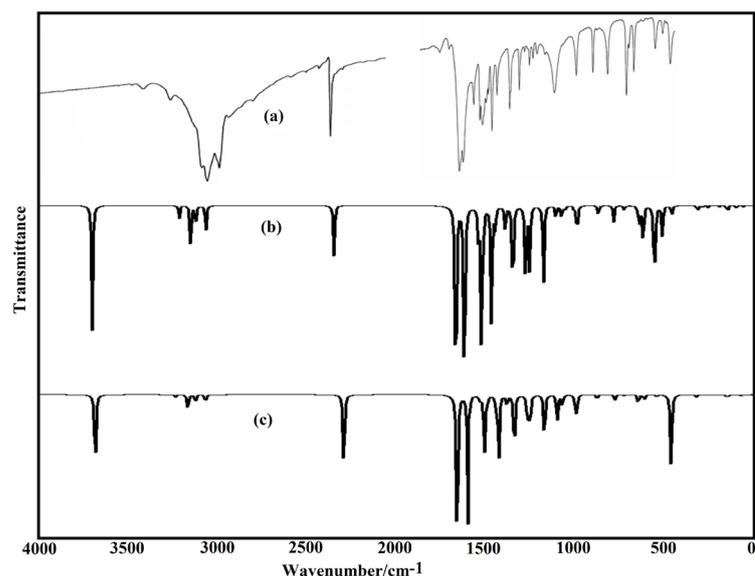
Figure 2. Comparison between the experimental Infrared spectra of: (a) 2-hydroxy-4,6-dimethylpyridine-3-carbonitrile from Ref [38] ith the corresponding theoretical in (b) gas phase and, (c) in aqueous solution at B3LYP/6-31G* level of theory.
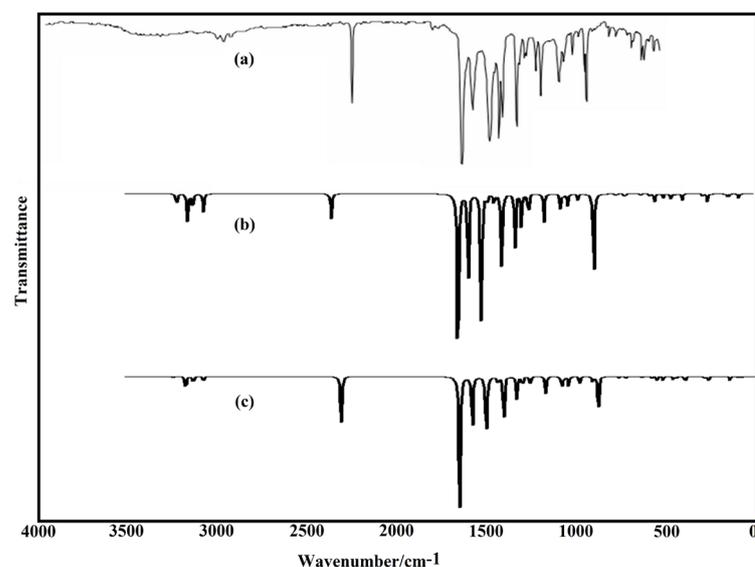
Figure 3. Comparison between the experimental Infrared spectra of: (a) 2-chloro-4,6-dimethylpyridine-3-carbonitrile from Ref [39] with the corresponding theoretical in (b) gas phase and, (c) in aqueous solution at B3LYP/6-31G* level of theory.

bands observed between 1095 and 1025 cm^{-1}. The twisting modes were not assigned because are predicted at 66 and 41 cm^{-1}.

C-C≡N modes. Here, the IR band at 2220 cm^{-1} is assigned to the C≡N stretching mode while the strong band at 720 cm^{-1} is assigned to the C2-C16 stretching mode, as observed in **Table 3**. The bending and out-of-plane deformation modes corresponding to the C2-C16 group are predicted at 236 and 138 cm^{-1} and, for this reason, they were not assigned.

Skeletal modes. The C-N stretching modes corresponding to the pyridine ring are predicted by the calcula-
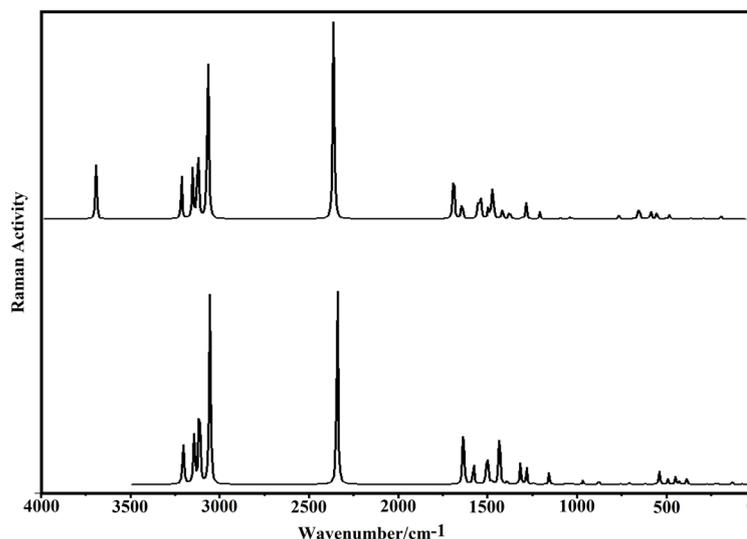
Figure 4. Comparison between the theoretical Raman spectra of the 2-hydroxy-4,6-dimethylpyridine-3-carbonitrile and 2-chloro-4,6-dimethylpyridine-3-carbonitrile derivatives at B3LYP/6-31G* level of theory.

tions in different regions. Hence, the IR bands at 1480 and 1140 cm^{-1} are associated respectively with those two C5-N7 and N7-C1 stretching modes while the strong band at 1375 cm^{-1}, is associated with the C-O stretching mode. Here, it is necessary to note that in aqueous solution there is a very important shifting in the wave numbers corresponding to those stretching modes, thus, the N7-C1 and C5-N7 stretching modes are predicted respectively at 1486 and 963 cm^{-1}, as observed in **Table 3**. This fact is related with the higher hydration of the (**2-OH**) derivative and with the increasing in the corresponding force constant values with the hydration as consequence of the increasing in the N7-C1 double bond character, as we will see later. Finally, the observed torsion and deformation modes of the pyridine ring are assigned as predicted by calculations and taking into account the assignments for similar molecules [45]-[49]. In this work, those modes are identified and assigned, as observed in **Table 3**.

4.2. Assignments for 2-Chloro-4,6-dimethylpyridine-3-carbonitrile

CH$_3$ modes. As in the (**2-OH**) derivative, the CH$_3$ ant symmetric and symmetric stretching modes are assigned between 3010 and 2975 cm^{-1} while the ant symmetric and symmetric CH$_3$ deformation modes bands are clearly assigned, as predicted by calculations, to the strong band at 1440 cm^{-1}. The four expected rocking modes are assigned to the bands between 1040 and 1000 cm^{-1}. In this derivative, the twisting modes were not assigned because both are predicted at 77 and 57 cm^{-1}. It is important to note that in this derivative the presence of the Cl atom in the structure shift the bands toward lower wave numbers, as observed in **Table 3**.

C-C≡N modes. Here, the C≡N stretching mode is assigned to the IR band at 2225 cm^{-1} while the weak band at 700 cm^{-1} is assigned to the C2-C16 stretching mode, as predicted by calculations.

In this derivative, with the hydration only is observed a shifting in the wave numbers related to the C5-N7 stretching mode, as indicated in **Table 3**. In (**2-Cl**), the C2-C16 bending mode is assigned to the weak band at 615 cm^{-1} while the corresponding out-of-plane deformation mode is predicted at 241 cm^{-1} and, for this, it mode is not assigned.

Skeletal modes. In this derivative, the C-N stretching modes corresponding to the pyridine ring are predicted by the calculations in the same regions, thus, both modes were assigned to the band and shoulder respectively at 1260 and 1250 cm^{-1}. The C-Cl stretching mode is predicted by calculations at 448 cm^{-1} and assigned at 440 cm^{-1}. The bending and out-of-plane deformation modes corresponding to the C1-Cl18 group are predicted at 230 and 160 cm^{-1}, hence, these modes were not assigned. Finally, in accordance with similar molecules [41]-[49] the torsion and deformation modes corresponding to the pyridine ring are assigned as predicted by calculations, as observed in **Table 3**.

Table 3. Observed and calculated wavenumbers (cm^{-1}) and assignments for the two studied cyanopyridine derivatives in gas phase and aqueous solution.

2-Hydroxy-4,6-dimethylpyridine-3-carbonitrile					2-Chloro-4,6-dimethylpyridine-3-carbonitrile				
Exp	Gas phase[a]		Aqueous solution[a]		Exp	Gas phase[a]		Aqueous solution[a]	
IR[b]	SQM[d]	Assignment	SQM[e]	Assignment	IR[c]	SQM[d]	Assignment	SQM[e]	Assignment
3350 s	3543	νO18-H19	3523	νO18-H19	3350 vw				
3280 w	3076	νC4-H6	3085	νC4-H6		3076	νC4-H6	3097	νC4-H6
3140 m	3016	ν_aCH$_3$(C8)	3050	ν_aCH$_3$(C12)	3010 w	3017	ν_aCH$_3$(C12)	3030	ν_aCH$_3$(C12)
	3015	ν_aCH$_3$(C12)	3015	ν_aCH$_3$(C8)		3017	ν_aCH$_3$(C8)	3030	ν_aCH$_3$(C8)
			2993	ν_aCH$_3$(C12)		2991	ν_aCH$_3$(C8)	2990	ν_aCH$_3$(C8)
2980 sh	2987	ν_aCH$_3$(C8)	2978	ν_aCH$_3$(C8)	2975 w	2986	ν_aCH$_3$(C12)	2989	ν_aCH$_3$(C12)
2950 s	2984	ν_aCH$_3$(C12)							
2925 vs	2932	ν_sCH$_3$(C8)	2931	ν_sCH$_3$(C12)	2920 w	2934	ν_sCH$_3$(C8)	2936	ν_sCH$_3$(C8)
2850 s	2931	ν_sCH$_3$(C12)	2928	ν_sCH$_3$(C8)	2850 w	2932	ν_sCH$_3$(C12)	2935	ν_sCH$_3$(C12)
2220 s	2250	νC16-N17	2232	νC16-N17	2225 m	2254	νC16-N17	2207	νC16-N17
			1699	νC3-C12					
1660 vs	1601	νC3-C4	1595	νC3-C4	1600 vs	1586	νC3-C4	1585	νC3-C4
1625 s			1536	νC2-C3					
1530 m	1548	νC2-C3	1486	νN7-C1	1535 m	1531	νC2-C3	1519	νC2-C3
1480 s	1484	νC5-N7	1455	δaCH$_3$(C8)					
1465 sh	1456	δaCH$_3$(C8)	1446	δaCH$_3$(C12)	1440 s	1457	δaCH$_3$(C8)	1442	νC5-N7
1460 s	1447	δaCH$_3$(C12)	1443	δaCH$_3$(C12)		1449	δaCH$_3$(C12)	1432	δaCH$_3$(C12)
1450 sh	1443	δaCH$_3$(C12)	1440	δaCH$_3$(C8)		1444	δaCH$_3$(C12)	1425	δaCH$_3$(C8)
1430 m	1440	δaCH$_3$(C8)	1433	νC1-C2		1438	δaCH$_3$(C8)	1424	δaCH$_3$(C12)
1375 s	1409	νC1-O18	1392	νC5-C8	1415 sh	1427	νC1-C2	1422	δaCH$_3$(C8)
1375 s	1379	δsCH$_3$(C12)	1370	δsCH$_3$(C12)	1380 s	1379	δsCH$_3$(C12)	1370	δsCH$_3$(C8)
1360 sh	1374	δsCH$_3$(C8)	1351	δsCH$_3$(C8)	1360 m	1375	δsCH$_3$(C8)	1362	δsCH$_3$(C12)
1340 m	1333	νC4-C5	1292	νC4-C5		1348	νC4-C5	1346	νC4-C5
1225 s	1285	δO18-H19	1222	νC2-C16	1260 s	1274	νN7-C1	1272	νN7-C1
					1250 sh	1241	νC5-N7	1245	νC1-C2
1215 m	1219	βC4-H6	1219	βC4-H6	1220 w	1215	βC4-H6	1216	βC4-H6
1175 sh	1205	νC1-C2			1160 m				
1140 s	1123	νN7-C1	1111	δO18-H19	1140 s	1130	βR$_1$	1131	βR$_1$
1095 w	1063	ρCH$_3$(C12)	1073	νC1-O18				1052	ρ'CH$_3$(C8)
1060 sh	1050	ρ'CH$_3$(C12)			1040 m	1049	ρ'CH$_3$(C12)	1048	ρ'CH$_3$(C12)
1055 m	1044	ρ'CH$_3$(C8)	1050	ρ'CH$_3$(C8) ρ'CH$_3$(C12)		1046	ρ'CH$_3$(C8)		
1025 w	1019	ρCH$_3$(C8)	1022	ρCH$_3$(C8)	1020	1025	ρCH$_3$(C12)	1031	ρCH$_3$(C8)
995 w			1007	γC4-H6	1000	1002	ρCH$_3$(C8)	1008	ρCH$_3$(C12)
960 w	967	βR$_1$	963	νC5-N7	950 w	940	νC5-C8	944	νC5-C8
925 s	934	νC5-C8	911	ρCH$_3$(C12)	910 w			892	γC4-H6
					880 sh	876	γC4-H6		
845 s	851	γC4-H6	795	τR$_1$	860 m	859	νC3-C12	847	νC1-Cl18
775 s	754	γC1-O18	740	τR$_1$	740 w	740	τR$_1$	736	τR$_1$
720 s	691	νC2-C16	672	βR$_1$	700 w	692	νC2-C16	696	νC2-C16
			634	γC1-O18					
640 s	626	γC5-C8	621	τR$_2$	620 w			620	δC2C16N17
615 m	618	βC5-C8	614	γC5-C8, τR$_1$	615 w	615	βC2-C16	614	γC5-C8
590 vw	588	νC3-C12			600 sh	606	γC5-C8		

Continued

580 w	581	γC3-C12							
			552	γC3-C12	550 w	559	γC3-C12	560	γC3-C12
					540 w	531	βR₂	531	νC3-C12
530 m	523	βR₂	518	βR₂					
495 m	502	τOH	492	τOH					
475 w	466	τwC2-C16	456	βC3-C12	480 w	470	τwC2-C16	484	τwC2-C16
460 m	447	δC2C16N17	443	βR₃	440 w	448	νC1-Cl18	447	βC5-C8
	424	βR₃				428	βC3-C12	430	βR₂
			401	τwC2-C16					
			385	βC5-C8		382	βR₃	379	βR₃
	303	βC1-O18	297	βC1-O18					
	277	βC3-C12				275	βC5-C8	279	βC3-C12
			241	γC2-C16		241	γC2-C16	249	γC2-C16
	236	γC2-C16				230	βC1-Cl18	230	βC1-Cl18
	223	τR₃	228	τR₃					
						209	τR₃	210	τR₃
	180	τR₁							
						160	γC1-Cl18	165	γC1-Cl18
	138	βC2-C16	148	βC2-C16 δC2C16N17		135	δC2C16N17	138	βC2-C16
			122	γC5-C8					
								95	τwCH₃(C12)
	82	τR₂	78	τwCH₃(C12)		77	τwCH₃(C12)	83	τwCH₃(C8)
	66	τwCH₃(C8)	74	τwCH₃(C8)		73	τR₂	73	τR₂
	41	τwCH₃(C12)				57	τwCH₃(C8)		

ν, stretching; δ, scissoring; wag and γ, wagging or out of plane deformation; ρ, rocking; τ, torsion, twist, twisting; a, antisymmetric; s, symmetric; R, ring; [a]This work, [b]From Ref [38], [c]From Ref [39], [d]From scaled quantum mechanics force field B3LYP/6-31G*, [e]From scaled quantum mechanics force field PCM/B3LYP/6-31G*.

5. Force Field

The force constants were calculated from the corresponding scaled force fields by using the Molvib program [37], as was described in Section 2. A comparison of the principal force constants for both derivatives in the two studied media are given in **Table 4**. In this study, the higher modifications are observed in the $f(\nu C\text{-}N)$, $f(\nu C\text{-}C)$ and $f(\nu C\text{-}O)$ force constants related to the (**2-OH**) derivative in aqueous solution because the values increasing notably with the hydration. In the (**2-Cl**) derivative only a slight increasing in some values and decreasing in other were observed with the hydration. Note that those higher values observed in the (**2-OH**) derivative in aqueous solution can not be attributed to the geometrical parameters because the C5-N7 and N7-C1 distances not change with the hydration, as observed in **Table 1** while, on the contrary, the C1-O8 distance is enlarged in solution. Thus, those values can be justified in part by the NBO results because there is a strong delocalization on the pyridine ring in the (**2-OH**) derivative that increasing its stability in aqueous solution due to the increasing in the double bonds character. The shifting of the bands attributed to the C5-N7, N7-C1 and C1-O8 stretching modes with the hydration also support the increasing of the corresponding force constants values.

6. Conclusion

The theoretical molecular structures of the 2-hydroxy-4,6-dimethylpyridine-3-carbonitrile and 2-chloro-4,6-dimethylpyridine-3-carbonitrile derivatives were determined in gas phase and in aqueous solution by using the B3LYP/6-31G* method employing the IEFPCM model. The complete assignments of the vibrational modes for both derivatives and the corresponding SQM force fields were obtained by using the B3LYP/6-31G* method. The predicted Raman spectra for the 2-hydroxy-4,6-dimethylpyridine-3-carbonitrile and 2-chloro-4,6-dimethylpyridine-3-carbonitrile derivatives have been reported by using the B3LYP/6-31G* method. Differences in

Table 4. Scaled force constants for the two studied cyanopyridine derivatives in gas and aqueous solution phases.

Force constant	B3LYP/6-31G^{*a}			
	2-Hydroxy-4,6-dimethylpyridine-3-carbonitrile		2-Chloro-4,6-dimethylpyridine-3-carbonitrile	
	Gas phase	PCM	Gas phase	PCM
$f(\nu O\text{-}H)$	7.03	7.01		
$f(\nu C\equiv N)$	17.77	17.91	17.82	17.06
$f(\nu C\text{-}N)$	7.25	13.56	7.22	7.10
$f(\nu C\text{-}C)_{A6}$	6.34	11.07	6.33	6.36
$f(\nu C\text{-}C)_{CH3}$	4.40	5.38	4.40	4.49
$f(\nu C\text{-}C)_{C\equiv N}$	5.46	6.22	5.42	5.48
$f(\nu C\text{-}O)$	6.45	14.29		
$f(\nu C\text{-}Cl)$			3.20	3.00
$f(\delta CH_3)$	0.54	0.69	0.54	0.53
$f(\delta C\text{-}O\text{-}H)$	0.79	2.30		
$f(\delta C\text{-}C\equiv N)$	0.34	0.48	0.33	0.36

ν, stretching; δ angle deformation. Units in mdyn Å^{-1} for stretching and mdyn Å rad^{-2} for angle deformations; [a]This work.

the studied properties for both derivatives in both media were justified by the molecular electrostatic potentials, atomic charges, bond orders, solvation energies, dipole moments, deslocalization energies and AIM analysis. A higher stability in aqueous solution for the 2-hydroxy-4,6-dimethylpyridine-3-carbonitrile derivative was found, which is supported in part by the NBO analysis, by a higher hydration of this derivative in solution due to its higher solvation energy and, by the higher force constant values. The analysis of the descriptors suggests that the OH group in the 2-hydroxy-4,6-dimethylpyridine-3-carbonitrile derivative reduces the HOMO-LUMO gap deactivating the ring while the calculated chemical hardness, chemical potential and global electrophilicity index values suggest a higher stability for the 2-chloro-4,6-dimethylpyridine-3-carbonitrile derivative and a better capability to accept electrons, as suggested by the AIM analysis. Here, the differences observed between the NBO and AIM results are probably due to that in the total energy only were considered those contributions with values higher than 20 kJ/mol. ^{1}H-NMR spectra observed for both derivatives were successfully compared with the calculated chemical shifts at the B3LYP/6-311++G** level of theory. The high value observed in the hydrogen chemical shift corresponding to the H atom of the OH group of 2-hydroxy-4,6-dimethylpyridine-3-carbonitrile, in relation to the calculated value, confirms the presence of the hydrogen bonds in solution for this derivative.

Acknowledgements

References

[1]   Márquez, M.B. and Brandán, S.A. (2014) A Structural and Vibrational Investigation on the Antiviral Deoxyribonucleoside Thymidine Agent in Gas and Aqueous Solution Phases. *International Journal of Quantum Chemistry*, **114**, 209-221. http://dx.doi.org/10.1002/qua.24545

[2]   Waly, M.A., EL-Hawary, I.I., Hamama, W.S. and Zoorob, H.H. (2013) Synthesis and Antitumor Evaluation of Some New Fused and Binary Pyridines. *Journal of Heterocyclic Chemistry*, **50**, E12-E17. http://dx.doi.org/10.1002/jhet.1020

[3]   Hawas, U.W., Al-Omar, M.A., Amr, A.E. and Hammam, A.G. (2011) Anticancer Activity of Some New Synthesized Tetrahydroquinoline and Tetrahydrochromene Carbonitrile Derivatives. *American Journal of Applied Sciences*, **8**, 945-952. http://dx.doi.org/10.3844/ajassp.2011.945.952

[4]   Amr, A.E., Abdel-Hafez, N.A., Mohamed, S.F. and Abdulla, M.M. (2009) Synthesis, Reactions, and Antiarrhythmic Activities of Some Novel Pyrimidines and Pyridines Fused with Thiophene Moiety. *Turkish Journal of Chemistry*, **33**, 421-432.

[5]   Abdel-Hafez, N.A., Mohamed, A.M., Amr, A.E. and Abdulla, M.M. (2009) Antiarrhythmic Activities of Some Newly Synthesized Tricyclic and Tetracyclic Thienopyridine Derivatives. *Scientia Pharmaceutica*, **77**, 539-553. http://dx.doi.org/10.3797/scipharm.0905-06

[6] Amr, A.E., Abdulla, M.M. (2006) Synthesis and Anti-Inflammatory Activities of New Cyanopyrane Derivatives Fused with Steroidal Nuclei. *Archiv der Pharmazie*, **339**, 88-95. http://dx.doi.org/10.1002/ardp.200500209

[7] Amr, A.E., Sayed, H.H. and Abdulla, M.M. (2005) Synthesis and Reactions of Some New Substituted Pyridine and Pyrimidine Derivatives as Analgesic, Anticonvulsant and Antiparkinsonian Agents. *Archiv der Pharmazie*, **338**, 433-440. http://dx.doi.org/10.1002/ardp.200500982

[8] Al-Omar, M.A. and Amr, A.E. (2010) Synthesis of Some New Pyridine-2,6-carboxamide-derived Schiff Bases as Potential Antimicrobial Agents. *Molecules*, **15**, 4711-4721. http://dx.doi.org/10.3390/molecules15074711

[9] Yamada, T., Takahashi, H. and Hatano, R. (1999) Nicotinoid Insecticidas and the Nicotine Acetylcholine Receptor. Yamamoto, I. and Casida, J.E., Eds., Springer-Verlag: Hong Kong, 149.

[10] Singh, T., Sharma, S., Srivastava, V.K. and Kumar, A. (2006) Synthesis and Biological Evaluation of Some Pyra- zo- linylpyridines and Pyrazolylpyridines. *Archiv der Pharmazie*, **339**, 24-31. http://dx.doi.org/10.1002/ardp.200500117

[11] Metwally, M.A., Abdel-Galil, E., Amer, F.A. and Abdallah, A.M. (2012) New Thiazolidinones, Thiazolines and Thiopyrimidines from 3,5-Diphenylcyclohex-2-enone. *American Journal of Organic Chemistry*, **2**, 28-34. http://dx.doi.org/10.5923/j.ajoc.20120201.06

[12] Durham, E.W., Siegfried, B.D. and Scharf, M.E. (2002) *In Vivo* and *in Vitro* Metabolism of Fipronil by Larvae of the European Corn Borer *Ostrinia nubilalis. Pest Management Science*, **58**, 799-804. http://dx.doi.org/10.1002/ps.523

[13] Thakkar, S.A. (2010) Studies on Bioactive Heterocycles and Other Moieties. Ph.D. Thesis, Saurashtra University, Rajkot.

[14] Mefetah, H., Giorgi, M. and Brouant, P. (1997) 2-Anilino-4,6-dimethylpyridine-3-carbonitrile, an Intermediate in the Synthesis of 5-Aminobenzo[b][1,8]naphthyridines. *Acta Crystallographica Section C*, **53**, 101-102. http://dx.doi.org/10.1107/S0108270196005276

[15] Laing, M., Sparrow, N. and Sommerville, P. (1971) The Crystal Structure of 4-Cyanopyridine. *Acta Crystallographica Section B*, **27**, 1986-1990. http://dx.doi.org/10.1107/S0567740871005211

[16] Wang, Y.C. (2012) 4-Cyano-Pyridinium Dihydrogen Phosphate-Isonicotinonitrile-Phospho-Ric Acid (1/1/1). *Acta Crystallographica Section E*, **68**, o1693-o1694.

[17] Daran, J., Jeannin, Y. and Martin, L.M. (1979) 3-Cyanopyridinium Tetrachloroferrate(III)-3-Cyanopyridine. *Acta Crystallographica Section B*, **35**, 3030-3032. http://dx.doi.org/10.1107/S0567740879011249

[18] Fan, W.J., Zhang, R.Q. and Liu, S. (2007) Computation of Large Systems with an Economic Basis Set: Structures and Reactivity Indices of Nucleic Acid Base Pairs from Density Functional Theory. *Journal of Computational Chemistry*, **28**, 967-974. http://dx.doi.org/10.1002/jcc.20670

[19] Chattaraj, P.K., Roy, D.R., Giri, S., Mukherjee, S., Subramanian, V., Parthasarathi, R., Bultinck, P. and Van Damme, S. (2007) An Atom Counting and Electrophilicity Based QSTR Approach. *Journal of Chemical Sciences*, **119**, 475-488. http://dx.doi.org/10.1007/s12039-007-0061-1

[20] Miertus, S., Scrocco, E. and Tomasi, J. (1981) Electrostatic Interaction of a Solute with a Continuum. A Direct Utilizaion of AB Initio Molecular Potentials for the Prevision of Solvent Effects. *Chemical Physics*, **55**, 117-129. http://dx.doi.org/10.1016/0301-0104(81)85090-2

[21] Rauhut, G. and Pulay, P. (1995) Transferable Scaling Factors for Density Functional Derived Vibrational Force Fields. *Journal of Physical Chemistry*, **99**, 3093-3100. http://dx.doi.org/10.1021/j100010a019

[22] Parr, R.G. and Pearson, R.G. (1983) Absolute Hardness: Companion Parameter to Absolute Electronegativity. *Journal of the American Chemical Society*, **105**, 7512-7516. http://dx.doi.org/10.1021/ja00364a005

[23] Reed, A.E., Curtis, L.A. and Weinhold, F. (1988) Intermolecular Interactions from a Natural Bond Orbital, Donor-Acceptor Viewpoint. *Chemical Reviews*, **88**, 899-926. http://dx.doi.org/10.1021/cr00088a005

[24] Glendening, E.D., Badenhoop, J.K., Reed, A.D., Carpenter, J.E. and Weinhold, F. (1996) NBO 3.1. Theoretical Chem- istry Institute, University of Wisconsin, Madison.

[25] Bader, R.F.W. (1990) Atoms in Molecules: A Quantum Theory. Oxford University Press, Oxford.

[26] Biegler-Köning, F., Schönbohm, J. and Bayles, D. (2001) AIM2000. *Journal of Computational Chemistry*, **22**, 545-559. http://dx.doi.org/10.1002/1096-987X(20010415)22:5<545::AID-JCC1027>3.0.CO;2-Y

[27] Nielsen, A.B. and Holder, A.J. (2009) Gauss View 5.0, User's Reference. GAUSSIAN Inc., Pittsburgh.

[28] Becke, A.D. (1993) Density-Functional Thermochemistry. III. The Role of Exact Exchange. *Journal of Chemical Physics*, **98**, 5648-5652. http://dx.doi.org/10.1063/1.464913

[29] Lee, C., Yang, W. and Parr, R.G. (1988) Development of the Colle-Salvetti Correlation-Energy Formula into a Functional of the Electron Density. *Physical Review B*, **37**, 785-789. http://dx.doi.org/10.1103/PhysRevB.37.785

[30] Frisch, M.J., Trucks, G.W., Schlegel, H.B., Scuseria, G.E., Robb, M.A., Cheeseman, J.R., Montgomery Jr., J.A., Vreven, T., Kudin, K.N., Burant, J.C., Millam, J.M., Iyengar, S.S., Tomasi, J., Barone, V., Mennucci, B., Cossi, M., Scalmani, G., Rega, N., Petersson, G.A., Nakatsuji, H., Hada, M., Ehara, M., Toyota, K., Fukuda, R., Hasegawa, J., Ishida, M., Nakajima, T., Honda, Y., Kitao, O., Nakai, H., Klene, M., Li, X., Knox, J.E., Hratchian, H.P., Cross, J.B., Adamo, C., Jaramillo, J., Gomperts, R., Stratmann, R.E., Yazyev, O., Austin, A.J., Cammi, R., Pomelli, C., Ochterski, J.W., Ayala, P.Y., Morokuma, K., Voth, G.A., Salvador, P., Dannenberg, J.J., Zakrzewski, V.G., Dapprich, S., Daniels, A.D., Strain, M.C., Farkas, O., Malick, D.K., Rabuck, A.D., Raghavachari, K., Foresman, J.B., Ortiz, J.V., Cui, Q., Baboul, A.G., Clifford, S., Cioslowski, J., Stefanov, B.B., Liu, G., Liashenko, A., Piskorz, P., Komaromi, I., Martin, R.L., Fox, D.J., Keith, T., Al-Laham, M.A., Peng, C.Y., Nanayakkara, A., Challacombe, M., Gill, P.M.W., Johnson, B., Chen, W., Wong, M.W., Gonzalez, C. and Pople, J.A. (2009) Gaussian 09, Revision A. 02. Gaussian, Inc., Pittsburgh.

[31] Marenich, A.V., Cramer, C.J. and Truhlar, D.G. (2009) Universal Solvation Model Based on Solute Electron Density and on a Continuum Model of the Solvent Defined by the Bulk Dielectric Constant and Atomic Surface Tensions. *Journal of Physical Chemistry B*, **113**, 6378-6396. http://dx.doi.org/10.1021/jp810292n

[32] Roldán, M.L., Ledesma, A.E., Raschi, A.B., Castillo, M.V., Romano, E. and Brandán, S.A. (2013) A New Experimental and Theoretical Investigation on the Structures of Aminoethyl Phosphonic Acid in Aqueous Medium Based on the Vibrational Spectra and DFT Calculations. *Journal of Molecular Structure*, **1041**, 73-81. http://dx.doi.org/10.1016/j.molstruc.2013.02.032

[33] Guzzetti, K., Brizuela, A.B., Romano, E. and Brandán, S.A. (2013) Structural and Vibrational Study on Zwitterions of l-Threonine in Aqueous Phase Using the FT-Raman and SCRF Calculations. *Journal of Molecular Structure*, **1045**, 171-179. http://dx.doi.org/10.1016/j.molstruc.2013.04.016

[34] Bichara, L.C. and Brandán, S.A. (2013) Hydration of Species Derived from Ascorbic Acid in Aqueous Solution. An Experimental and Theoretical Study by Using DFT Calculations. *Journal of Molecular Liquids*, **181**, 34-43. http://dx.doi.org/10.1016/j.molliq.2013.02.009

[35] Ugliengo, P. (1998) MOLDRAW Program. University of Torino, Dipartimento Chimica IFM, Torino.

[36] Besler, B.H., Merz Jr., K.M. and Kollman, P.A. (1990) Atomic Charges Derived from Semiempirical Methods. *Journal of Computational Chemistry*, **11**, 431-439. http://dx.doi.org/10.1002/jcc.540110404

[37] Sundius, T. (2002) Scaling of *ab initio* Force Fields by MOLVIB. *Vibrational Spectroscopy*, **29**, 89-95. http://dx.doi.org/10.1016/S0924-2031(01)00189-8

[38] FTIR spectrum of 2-Hydroxy-4,6-dimethylpyridine-3-carbonitrile from Aldrich Nº 303A99F2d01.pdf.

[39] FTIR spectrum of 3-Pyridinecarbonitrile, 2-chloro-4,6-dimethyl-from LookChem Nº 14237-71-9.

[40] Contreras, C.D., Montejo, M., López González, J.J., Zinczuk, J. and Brandán, S.A. (2011) Structural and Vibrational Analyses of 2-(2-Benzofuranyl)-2-imidazoline. *Journal of Raman Spectroscopy*, **42**, 108-116. http://dx.doi.org/10.1002/jrs.2659

[41] Contreras, C.D., Ledesma, A.E., Zinczuk, J. and Brandán, S.A. (2011) Vibrational Study of Tolazoline Hydrochloride by Using FTIR-Raman and DFT Calculations. *Spectrochimica Acta Part A*, **79**, 1710-1714. http://dx.doi.org/10.1016/j.saa.2011.05.041

[42] Contreras, C.D., Montejo, M., López González, J.J., Zinczuk, J. and Brandán, S.A. (2011) Structural and Vibrational Analyses of 2-(-2-Benzofuranyl)-2-imidazoline. *Journal of Raman Spectroscopy*, **42**, 108-116.

[43] Romano, E., Raschi, A.B., Benavente, A. and Brandán, S.A. (2011) Structural Analysis, Vibrational Spectra and Coordinated Normal of 2R-(-)-6-Hydroxytremetone. *Spectrochimica Acta Part A*, **84**, 111-116. http://dx.doi.org/10.1016/j.saa.2011.09.011

[44] Leyton, P., Brunet, J., Silva, V., Paipa, C., Castillo, M.V. and Brandán, S.A. (2012) An Experimental and Theoretical Study of l-Tryptophan in an Aqueous Solution, Combining Two-Layered ONIOM and SCRF Calculations. *Spectrochimica Acta Part A*, **88**, 162-170. http://dx.doi.org/10.1016/j.saa.2011.12.023

[45] Lizarraga, E., Romano, E., Rudyk, R., Catalán, C.A.N. and Brandán, S.A. (2012) Structural Study, Coordinated Normal Analysis and Vibrational Spectra of 4-Hydroxy-3-(3-methyl-2-butenyl)acetophenone. *Spectrochimica Acta Part A*, **97**, 202-208. http://dx.doi.org/10.1016/j.saa.2012.06.004

[46] Leyton, P., Paipa, C., Berrios, A., Zárate, A., Fuentes, S., Castillo, M.V. and Brandán, S.A. (2013) Structural Study and Characterization of the Dipeptide 2-[[5-Amino-5-oxo-2-(phenylmethoxycarbonylamino) Pentanoyl] Amino] Acetic Acid by Vibrational Spectroscopy and DFT Calculations. *Journal of Molecular Structure*, **1031**, 110-118. http://dx.doi.org/10.1016/j.molstruc.2012.07.042

[47] Piro, O.E., Echeverría, G.A., Lizarraga, E., Romano, E., Catalán, C.A.N. and Brandán, S.A. (2013) Molecular Structure of 4-hidroxy-3-(3-methyl-2-butenyl) Acetophenone, a Plant Antifungal, by X-Ray Diffraction, DFT Calculation, and NMR and FTIR Spectroscopy. *Spectrochimica Acta Part A*, **101**, 196-203. http://dx.doi.org/10.1016/j.saa.2012.09.086

[48] Romano, E., Brizuela, A.B., Guzzetti, K. and Brandán, S.A. (2013) An Experimental and Theoretical Study on the

Hydration in Aqueous Medium of the Antihypertensive Agent Tolazoline Hydrochloride. *Journal of Molecular Structure*, **1037**, 393-401. http://dx.doi.org/10.1016/j.molstruc.2013.01.028

[49] Lizarraga, E., Romano, E., Raschi, A.B., Leyton, P., Paipa, C., Catalán, A.C.N. and Brandán, S.A. (2013) A Structural and Vibrational Study of Dehydrofukinone Combining FTIR, FTRaman, UV-Visible and NMR Spectroscopies with DFT Calculations. *Journal of Molecular Structure*, **1048**, 331-338. http://dx.doi.org/10.1016/j.molstruc.2013.05.067

Supporting Information

Table S1. Total (E) and relative (ΔE) energies and dipole moment (μ) for the two studied cyanopyridine derivatives.

B3LYP/6-31G*		
Compound	E (Hartrees)	μ (D)
Gas phase		
2-Hydroxy-4,6-dimethylpyridine-3-carbonitrile	−494.3993	5.12
2-Chloro-4,6-dimethylpyridine-3-carbonitrile	−878.7631	5.53
Aqueous solution		
2-Hydroxy-4,6-dimethylpyridine-3-carbonitrile	−494.4116	7.07
2-Chloro-4,6-dimethylpyridine-3-carbonitrile	−878.7721	7.95

Table S2. Molecular electrostatic potential (in a.u.) for the two studied cyanopyridine derivatives.

B3LYP/6-31G*					
2-Hydroxy-4,6-dimethylpyridine-3-carbonitrile			2-Chloro-4,6-dimethylpyridine-3-carbonitrile		
Atoms	Gas phase	PCM	Atoms	Gas phase	PCM
1 C	−14.619	−14.619	1 C	−14.617	−14.617
2 C	−14.690	−14.691	2 C	−14.671	−14.672
3 C	−14.688	−14.688	3 C	−14.676	−14.675
4 C	−14.723	−14.723	4 C	−14.708	−14.708
5 C	−14.673	−14.673	5 C	−14.662	−14.662
6 H	−1.085	−1.085	6 H	−1.073	−1.072
7 N	−18.349	−18.348	7 N	−18.336	−18.335
8 C	−14.726	−14.726	8 C	−14.721	−14.720
9 H	−1.098	−1.098	9 H	−1.093	−1.092
10 H	−1.098	−1.098	10 H	−1.093	−1.092
11 H	−1.101	−1.101	11 H	−1.095	−1.095
12 C	−14.720	−14.720	12 C	−14.711	−14.711
13 H	−1.094	−1.094	13 H	−1.085	−1.084
14 H	−1.098	−1.098	14 H	−1.085	−1.084
15 H	−1.094	−1.094	15 H	−1.089	−1.088
16 C	−14.716	−14.717	16 C	−14.704	−14.704
17 N	−18.377	−18.377	17 N	−18.364	−18.364
18 O	−22.261	−22.262	18 Cl	−64.367	−64.368
19 H	−0.948	−0.948			

Table S3. Atomic charges for the two studied cyanopyridine derivatives.

B3LYP/6-31G*									
2-Hydroxy-4.6-dimethylpyridine-3-carbonitrile					2-Chloro-4.6-dimethylpyridine-3-carbonitrile				
Atoms	Gas phase		PCM		Atoms	Gas phase		PCM	
	MK' charges	NPA	MK' charges	NPA		MK' charges	NPA	MK' charges	NPA
1 C	0.796	0.604	0.789	0.604	1 C	0.371	0.247	0.381	0.252
2 C	−0.600	−0.258	−0.590	−0.258	2 C	−0.278	−0.225	−0.300	−0.227
3 C	0.557	0.070	0.552	0.070	3 C	0.470	0.067	0.484	0.069
4 C	−0.714	−0.301	−0.708	−0.300	4 C	−0.639	−0.273	−0.660	−0.274
5 C	0.765	0.259	0.759	0.258	5 C	0.739	0.255	0.777	0.255
6 H	0.222	0.244	0.220	0.243	6 H	0.217	0.247	0.218	0.247
7 N	−0.775	−0.538	−0.769	−0.534	7 N	−0.591	−0.462	−0.602	−0.460
8 C	−0.545	−0.703	−0.541	−0.703	8 C	−0.585	−0.705	−0.624	−0.705

Continued

9	H	0.158	0.256	0.157	0.256	9	H	0.170	0.261	0.178	0.261
10	H	0.158	0.256	0.157	0.256	10	H	0.170	0.261	0.178	0.261
11	H	0.130	0.238	0.129	0.237	11	H	0.141	0.238	0.150	0.238
12	C	−0.419	−0.701	−0.415	−0.701	12	C	−0.454	−0.702	−0.452	−0.702
13	H	0.129	0.262	0.127	0.262	13	H	0.148	0.264	0.146	0.264
14	H	0.120	0.244	0.120	0.244	14	H	0.148	0.264	0.146	0.264
15	H	0.129	0.262	0.127	0.262	15	H	0.129	0.247	0.131	0.247
16	C	0.514	0.277	0.506	0.276	16	C	0.336	0.269	0.348	0.268
17	N	−0.478	−0.304	−0.476	−0.303	17	N	−0.415	−0.284	−0.418	−0.282
18	O	−0.571	−0.672	−0.571	−0.675	18	Cl	−0.078	0.030	−0.083	0.023
19	H	0.427	0.503	0.427	0.504						

Table S4. Wiberg indexes for the two studied cyanopyridine derivatives.

B3LYP/6-31G*					
2-Hydroxy-4,6-dimethylpyridine-3-carbonitrile			2-Chloro-4,6-dimethylpyridine-3-carbonitrile		
Atoms	Gas phase	PCM	Atoms	Gas phase	PCM
1 C	3.898	3.899	1 C	4.014	4.014
2 C	3.965	3.965	2 C	3.976	3.975
3 C	3.990	3.990	3 C	3.991	3.990
4 C	3.935	3.935	4 C	3.937	3.937
5 C	3.974	3.975	5 C	3.976	3.976
6 H	0.942	0.942	6 H	0.940	0.941
7 N	3.073	3.073	7 N	3.112	3.113
8 C	3.835	3.835	8 C	3.832	3.832
9 H	0.936	0.936	9 H	0.934	0.933
10 H	0.936	0.936	10 H	0.934	0.933
11 H	0.945	0.945	11 H	0.944	0.944
12 C	3.822	3.822	12 C	3.819	3.819
13 H	0.933	0.933	13 H	0.931	0.931
14 H	0.942	0.941	14 H	0.931	0.931
15 H	0.933	0.933	15 H	0.940	0.940
16 C	4.005	4.006	16 C	4.006	4.006
17 N	3.026	3.026	17 N	3.031	3.031
18 O	1.975	1.969	18 Cl	1.259	1.251
19 H	0.749	0.748			

Table S5. Main delocalization energy (in kJ/mol) for the two studied cyanopyridine derivatives.

B3LYP/6-31G*					
2-Hydroxy-4,6-dimethylpyridine-3-carbonitrile			2-Chloro-4,6-dimethylpyridine-3-carbonitrile		
Delocalization	Gas phase	PCM	Delocalization	Gas phase	PCM
$\sigma(2)$C1-N7 → σ^*C4-C5	120.13	117.79	$\sigma(2)$C1-N7 → σ^*C2-C3	42.55	43.18
	0	0	$\sigma(2)$C1-N7 → σ^*C4-C5	102.24	99.9
$\sigma(2)$C2-C3 → σ^*C1-N7	140.57	140.24	$\sigma(2)$C2-C3 → σ^*C1-N7	131.88	134.55
$\sigma(2)$C2-C3 → σ^*C4-C5	52.46	53.38	$\sigma(2)$C2-C3 → σ^*C4-C5	57.14	57.56
$\sigma(2)$C2-C3 → σ^*C16-N17	84.56	86.11	$\sigma(2)$C2-C3 → σ^*C16-N17	79.08	80.09
$\sigma(2)$C4-C5 → σ^*C1-N7	52.08	51.08	$\sigma(2)$C4-C5 → σ^*C1-N7	67.13	64.5
$\sigma(2)$C4-C5 → σ^*C2-C3	123.64	123.31	$\sigma(2)$C4-C5 → σ^*C2-C3	120.34	120.17
$\sigma(1)$C16-N17 → σ^*C2-C16	25.62	25.87	$\sigma(1)$C16-N17 → σ^*C2-C16	26.08	26.25

Continued

$\sigma(2)$C16-N17 $\to \sigma^*$C1-C2	14.29	14.46	$\sigma(2)$C16-N17 $\to \sigma^*$C1-C2	14.21	14.34
$\sigma(3)$C16-N17 $\to \sigma^*$C2-C3	30.72	31.64	$\sigma(3)$C16-N17 $\to \sigma^*$C2-C3	32.23	32.94
$\sigma(1)$O18-H19 $\to \sigma^*$C1-C2	25.12	23.37		0	0
$\Delta ET_{\pi \to \pi^*}$	669.19	667.25	$\Delta ET_{\pi \to \pi^*}$	672.88	673.48
LP(1)N7 $\to \sigma^*$C1-C2	49.78	49.28	LP(1)N7 $\to \sigma^*$C1-C2	47.52	47.48
LP(1)N7 $\to \sigma^*$C2-C16	53.17	53.63	LP(1)N7 $\to \sigma^*$C2-C16	54.09	54.55
LP(2)O18 $\to \sigma^*$C1-N7	166.78	165.56	LP(3)Cl18 $\to \sigma^*$C1-N7	68.34	65.83
$\Delta ET_{LP \to \sigma^*}$	269.73	268.47	$\Delta ET_{LP \to \sigma^*}$	169.95	167.86
$\sigma^*(2)$C1-N7 $\to \sigma^*$C2-C3	644.76	673.02	$\sigma^*(2)$C1-N7 $\to \sigma^*$C2-C3	541.81	591.26
$\sigma^*(2)$C1-N7 $\to \sigma^*$C4-C5	420.42	426.61	$\sigma^*(2)$C1-N7 $\to \sigma^*$C4-C5	378.67	384.18
$\sigma^*(2)$C2-C3 $\to \sigma^*$C16-N17	82.72	85.15	$\sigma^*(2)$C2-C3 $\to \sigma^*$C16-N17	79.75	81.43
$\Delta ET_{\sigma^* \to \sigma^*}$	1147.9	1184.78	$\Delta ET_{\sigma^* \to \sigma^*}$	1000.23	1056.87
ΔE_{Total}	2086.82	2120.5	ΔE_{Total}	1843.06	1898.21

Table S6. Analysis of the ring critical points (RCP) for the two studied cyanopyridine derivatives.

	B3LYP/6-31G*			
Parameter (a.u.)	2-Hydroxy-4,6-dimethylpyridine-3-carbonitrile		2-Chloro-4,6-dimethylpyridine-3-carbonitrile	
	Gas phase	PCM	Gas phase	PCM
$\rho(r_c)$	0.0217	0.0217	0.0220	0.0220
$\nabla^2 \rho(r_c)$	0.1694	0.1694	0.1717	0.1719
λ_1	−0.0171	−0.0171	−0.0176	−0.0176
λ_2	0.0876	0.0876	0.0883	0.0874
λ_3	0.0988	0.0988	0.1009	0.1021
$|\lambda_1|/\lambda_3$	0.1730	0.1730	0.1744	0.1724

Table S7. Calculated HOMO and LUMO orbitals, energy band gap, chemical potential (μ), electronegativity (χ), global hardness (η), global softness (S) and global electrophilicity index (ω) for the two studied cyanopyridine derivatives.

	B3LYP/6-31G*			
	2-Hydroxy-4,6-dimethylpyridine-3-carbonitrile		2-Chloro-4,6-dimethylpyridine-3-carbonitrile	
Orbitals	Gas phase	PCM	Orbitals	Gas phase	PCM
HOMO (39) (eV)	−6.7102	−6.7025	HOMO (43) (eV)	−7.2680	−7.2762
LUMO (40) (eV)	−1.5401	−1.5571	LUMO (44) (eV)	−1.8776	−1.9073
GAP (eV)	−5.1701	−5.1454	GAP (eV)	−5.3904	−5.3689

	2-Hydroxy-4,6-dimethylpyridine-3-carbonitrile		2-Chloro-4,6-dimethylpyridine-3-carbonitrile	
Descriptors	Gas phase	PCM	Gas phase	PCM
$\chi = -[E(LUMO) - E(HOMO)]/2$ (eV)	−2.5850	−2.5727	−2.6952	−2.6844
$\mu = [E(LUMO) + E(HOMO)]/2$ (eV)	−4.1251	−4.1251	−4.5728	−4.5917
$\eta = [E(LUMO) - E(HOMO)]/2$ (eV)	2.5850	2.5727	2.6952	2.6844
$S = 1/2\eta$ (eV)	0.1934	0.1943	0.1855	0.1862
$\omega = \mu^2/2\eta$ (eV)	3.2914	3.3071	3.8792	3.9271

Table S8. Observed and calculated hydrogen chemical shifts (δ, in ppm).

Atoms	2-Hydroxy-4,6-dimethylpyridine-3-carbonitrile		2-Chloro-4,6-dimethylpyridine-3-carbonitrile	
	Calc.[a]	Exp[b]	Calc.[a]	Exp[b]
H6	6.588	6.100 s, H, pyridyl	6.324	7.000 s, H, pyridyl
H9	2.511	2.300 s, 3H, CH3-C=C	2.240	2.400 s, 3H, CH3-C=C
H10	2.511	2.300 s, 3H, CH3-C=C	2.240	2.400 s, 3H, CH3-C=C
H11	2.030	2.300 s, 3H, CH3-C=C	1.519	2.400 s, 3H, CH3-C=C

Continued

H13	2.511	2.400 s, 3H, CH3-C=N	2.240	2.500 s, 3H, CH3-C=N
H14	1.926	2.400 s, 3H, CH3-C=N	2.240	2.500 s, 3H, CH3-C=N
H15	2.511	2.400 s, 3H, CH3-C=N	1.519	2.500 s, 3H, CH3-C=N
H19	5.750	12.200 s, H, OH		
RMSD	**0.81**		**0.22**	

[a]GIAO/B3LYP/6-311++G[**] Ref. to TMS; [b]Experimental dissolved in CDCl$_3$ [2]. TMS as reference.

Table S9. Observed and calculated hydrogen chemical shifts (δ, in ppm).

Atoms	2-Hydroxy-4,6-dimethylpyridine-3-carbonitrile	2-Chloro-4,6-dimethylpyridine-3-carbonitrile
	Calculated.[a]	Calculated.[a]
C1	188.021	147.974
C2	113.798	97.364
C3	181.849	141.92
C4	138.881	109.563
C5	185.507	148.577
C8	43.145	17.296
C12	39.429	14.417
C16	136.111	96.088

[a]GIAO/B3LYP/6-311++G[**] Ref. to TMS.
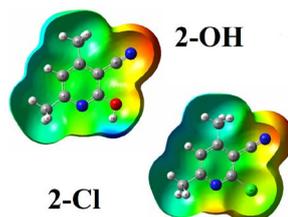
Figure S1. Calculated electrostatic potential surfaces on the molecular surfaces of 2-OH and 2-Cl derivatives. Color ranges, in au: from red −0.05 to blue +0.05. B3LYP functional and 6-31G[*] basis set. Isodensity value of 0.005.
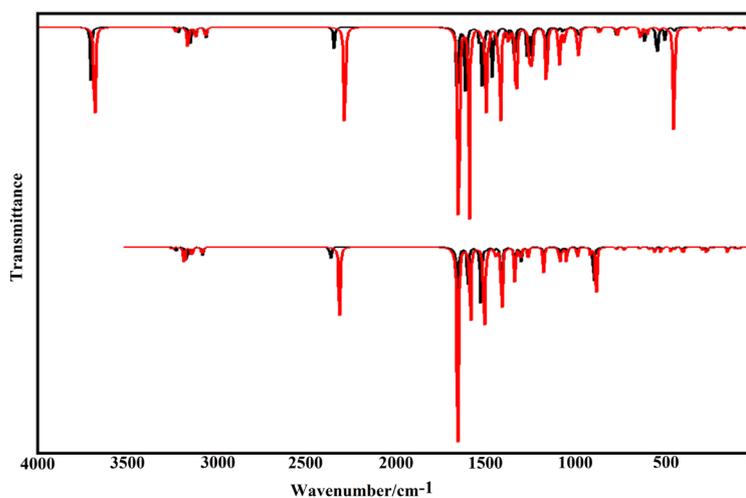
Figure S2. Comparison between the theoretical infrared spectra in gas phase (black color) and in aqueous solution (red color) at B3LYP/6-31G[*] level of theory for 2-hydroxy-4,6-dimethylpyridine-3-carbonitrile (upper) and 2-chloro-4,6-dimethylpyridine-3-carbonitrile (bottom).